Plausible Variable-head Tests Initiated with Continuous Pumping in Monitoring Wells

L. Zhang, R.P. Chapuis
École Polytechnique, Montréal, Québec, Canada

ABSTRACT
The variable-head (VH) test is initiated by suddenly injecting or withdrawing a volume of water and recording the water level recovery in the monitoring well (MW). A slug or solid rod is added to displace water, which yields a falling recovery of water level. For a rising-head test, a slug of water is removed by extracting the sunk rod or a bailer. A pump can also be used to either inject or remove water, but it is more difficult to practise because it must be conducted very quickly. Seven real and numerical tests in aquifers were considered to be variable-head tests. However, the water recovery in the MW occurred after 15- to 40-min pumping, which are actually constant-head (CH) tests. The paper proves that the interpretation methods for the VH test are applicable to the recovery data of CH test. Five tests have different K_{CH} and K_{VH} values, and present curved or scattered velocity plots instead of straight lines, which is indicative of poorly installed MWs.

RÉSUMÉ
L'essai à charge variable est initié en injectant ou en retirant soudainement un volume d'eau et en enregistrant la récupération du niveau d'eau dans le tube. Un bouchon ou une tige solide est ajouté pour déplacer l'eau, ce qui produit un essai à niveau descendant. Pour un essai à niveau remontant, un bouchon d'eau est retiré en extrayant la tige coulée ou l'écope. Une pompe peut également être utilisée pour injecter ou retirer de l'eau, mais il est plus difficile de l'utiliser car elle doit être effectuée très rapidement. Sept essais réels et numériques dans les aquifères ont été considérés comme des essais à charge variable. Cependant, la récupération d'eau dans le tuyau s'est produite après un pompage de 15 à 40 minutes, qui sont en fait des essais à charge constante. L'article prouve que les méthodes d'interprétation pour le test VH sont applicables aux données de récupération du test CH. Cinq essais ont des valeurs K_{CH} et K_{VH} différentes, et présentent des courbes de vitesse incurvées ou dispersées au lieu de droites, ce qui est indicatif de MW mal installés.

1 INTRODUCTION

The variable-head (VH) or slug test, is frequently used to assess the hydraulic properties of the aquifer because it is easy and fast to apply in the field. It is initiated by a sudden increase or decrease of water volume, which corresponds to a falling- or rising-head test, respectively (ASTM D4044 2015, CAN/BNQ 2501-135 2014). The falling recovery of water level can be caused by inserting a slug or solid rod to displace water. A volume of water is removed by extracting the sunk rod or a bailer, which starts the rising-head test. If a pump is used to add or remove water in the pipe, the addition or removal must be conducted quickly. As a longer pumping duration represents a constant flowrate test (ISO 22282-2, 2012), also known as a constant-head (CH) test (Cassan 2005, CAN/BNQ 2501-135 2014).

The paper was inspired by an inquiry from a field practitioner asking why the velocity graphs he plotted did not display straight lines for several VH tests. The so-called VH tests, however, were found to be the recovery phases after groundwater sampling, which pumps water constantly for a period of time, rather than the real VH tests.

Therefore, the first question is can we use the interpretation methods of VH test to deal with the recovery data of the CH test? If yes, the second question is, does the velocity plot still present a straight line for a good CH recovery test?

The paper first presents the theoretical evidence to apply the interpretation methods of VH tests on the recovery data of CH tests. A total number of five examples that have curved or scattered velocity plots are presented subsequently. The K_{CH} is used to refer the hydraulic conductivity calculated by the interpretation method of CH test. It is determined through the provided constant flowrate (Q) and hydraulic head difference (H_c). Meanwhile, the test data are analyzed by the interpretation methods of VH tests: Hvorslev's semi-log plot (Hvorslev 1951), velocity graph (Chapuis et al. 1981), and *Z-t* method (Chiasson 2005). The yielded hydraulic conductivity is termed K_{VH}. The values of K_{CH} and K_{VH} are then compared. In addition, another two CH tests performed in MWs of good conditions are analyzed in the same way. The results are compared with those of the five previous tests.

2 THEORETICAL SOLUTIONS

2.1 Interpretation of hydraulic conductivity

In a CH test, the constant discharge/injection rate Q generates a constant hydraulic head difference H_c when the test reaches equilibrium. With the knowledge of the shape factor $c=2\pi L/\ln(2L/D)$ (Hvorslev 1951), we know from the Lefranc's solution (Lefranc 1936, 1937) that the flow rate through the water injection zone (Q_s) has found to be related to the applied hydraulic head (H_c) as follows:

$$Q_s = cKH_c \quad [1]$$

where Q_s = Q in steady state. The saturated hydraulic conductivity K in the aquifer is interpreted by

$$K = \frac{Q}{cH_c} \quad [2]$$

If the recovery of a CH test is considered as a VH test with a rising/falling water level in the MW, the K value can be determined from the Hvorslev's semi-log plot, expressed as

$$\ln\left(\frac{H_1}{H_2}\right) = -\frac{cK}{S_{inj}}(t_1 - t_2) \quad [3]$$

where the hydraulic heads H_1 and H_2 at respective times, t_1 and t_2 appear as a straight line if there is no piezometric error, and S_{inj} is the internal area of the MW. Therefore,

$$K = -P_1 \cdot \frac{S_{inj}}{c} \quad [4]$$

in which P_1 is the slope of the straight line represented by eq.3. If a piezometric error H_0 exists, the semi-log plot can be upward or downward curved (Chapuis 1998, 2015, 2017). The H_0 value is estimated by either the velocity graph (eq.5) or the Z-t methods (Chiasson 2005). The detailed calculation processes of the two methods were presented by Zhang et al. (2018 a, b)

$$H = -\frac{S_{inj}}{cK}\frac{dH}{dt} + H_0 \quad [5]$$

The K value is expressed as

$$K = \frac{1}{P_2} \cdot \frac{S_{inj}}{c} \quad [6]$$

where P_2 is the slope of the straight velocity plot referred by eq. 5.

2.2 Theoretical examination

The section explains why the interpretation methods of a VH test can be used for a CH test in theory. Cassan (2005) presented the interpretation of transient state of the CH test. In the transient phase, $Q_s \neq Q$, and the relative flow rate in the pipe is $Q - Q_s$. Therefore, the variation of the water level (dH) in the well pipe with an internal area of S_{inj} during the time dt, corresponds to the movement of a volume of water:

$$(Q - Q_s)dt = S_{inj}dH \quad [7]$$

Substituting eq. 1 into eq. 7, the equation can be rewritten as:

$$\frac{dH}{\frac{cKH}{S_{inj}} - \frac{Q}{S_{inj}}} = -dt \quad [8]$$

which is the differential equation governs the flow in the transient state. Integrating both sides from time t_i to t and from head H_i to H, the equation becomes:

$$H = \frac{Q}{cK} + \left(H_i - \frac{Q}{cK}\right) \cdot e^{\left[-\frac{cK}{S_{inj}}(t - t_i)\right]} \quad [9]$$

The hydraulic head difference H of the injection zone reaches a limit of H_c = $Q/(cK)$ when t tends to infinity, which indicates that the representative curve of eq. 9 has an asymptote parallel to the x-axis. Therefore, the asymptote corresponds to the steady state where the Q is equivalent to Q_s. When the time and head are recorded at the time we start the pump (t_i and H_i are equal to 0), eq. 9 is simplified to:

$$H = \frac{Q}{cK}\left(1 - e^{\left(-\frac{cK}{S_{inj}}t\right)}\right). \quad [10]$$

It is observed that the ordinate of the asymptote is still H_c = $Q/(cK)$, and the slope of the tangent at the origin is calculated as Q/S_{inj}.

The recovery phase after the steady state, which represents a test at zero flow after the constant flow is stopped. Because Q = 0, eq. 9 becomes:

$$H = H_i e^{\left[-\frac{cK}{S_{inj}}(t - t_i)\right]} \quad [11]$$

where H_i and t_i refer to the water head in the well pipe and the time, respectively, at the moment the pump stops. Eq. 11 can be rewritten as:

$$\ln\left(\frac{H}{H_i}\right) = -\frac{cK}{S_{inj}}(t - t_i) \quad [12]$$

which is the same as the Hvorslev's semi-log plot represented by eq. 3.

The relative velocity of the water flow in pipe from eq. 7 is:

$$v = \frac{Q - Q_s}{S_{inj}} = \frac{dh}{dt} \quad [13]$$

The ratio Q/S_{inj} represents the maximum instantaneous velocity of the water in the pipe, from the start-up of the pumps, before the water movement into the soil begins. Therefore, the initial velocity $v_i = Q/S_{inj}$ at time t = 0 for a zero head. The differential equation (eq. 8) is written as:

$$v = v_i - \frac{cK}{S_{inj}} H \qquad [14]$$

where the relative velocity (v) and the corresponding head difference (H) during dt are calculated by the two consecutive measurements:

$$H = \frac{H_{j+1} + H_j}{2} \text{ and } v = \frac{H_{j+1} + H_j}{t_{j+1} - t_j}.$$

As soon as the pump is stopped, the hydraulic head, which has reached a maximum value of H_c, begins to dissipate and the injection/discharge flow rate becomes zero. As Q = 0, the initial velocity v_i = 0 in eq. 14, we have

$$v = -\frac{cK}{S_{inj}} H \qquad [15]$$

which can be transformed into the eq. 5 of velocity graph by adding the piezometric correction.

Therefore, eqs. 12 and 15 prove that the VH test methods of Hvoslev and the velocity graph can be used to interpret the recovery phases of a CH discharge/injection test, groundwater sampling, and pumping test.

3 EXAMPLES OF POORLY INSTALLED WELLS

The five examples present the recovery data after groundwater sampling. The first three tests were performed in a sand aquifer, whereas the last two were in a till (silty sand) layer. The flow rates, steady-state head differences, shape factors and inside cross-sectional areas of MWs are summarized in Table 1. The information of Q and H_c are missing for examples 4 and 5. The tests are interpreted by the CH test method first, and then compared with the VH test methods. We use K_{VH1}, K_{VH2}, and K_{VH3} to refer to the K_{VH} values estimated from the semi-log graph, velocity graph and optimized semi-log graph by the Z-t method, respectively.

Table 1. Several information of the examples.

example	pumping rate Q (cm^3/s)	head difference H_c (cm)	internal area S_{inj} (cm^2)	shape factor c (cm)
1	181.0	179.5	20.3	384.6
2	540.7	220.4	20.3	545.6
3	83.8	3.7	20.3	473.2
4	--	--	5.1	538.8
5	--	--	5.1	538.8
6	7.6	15.7	9.3	221.6
7	609	100	21.2	244.1

3.1 Example 1

The MW has a 305 cm long screen but only 225 cm were immersed before the sampling and testing. The data was collected during recovery after 38 minutes of pumping at a rate of 10.86 L/min (see Figure 1), which generated a constant head difference of 179.5 cm. The hydraulic conductivity K_{CH} is 2.6 x 10^{-3} cm/s. The semi-log and velocity graphs are plotted in the same graph on primary and secondary axes, respectively.

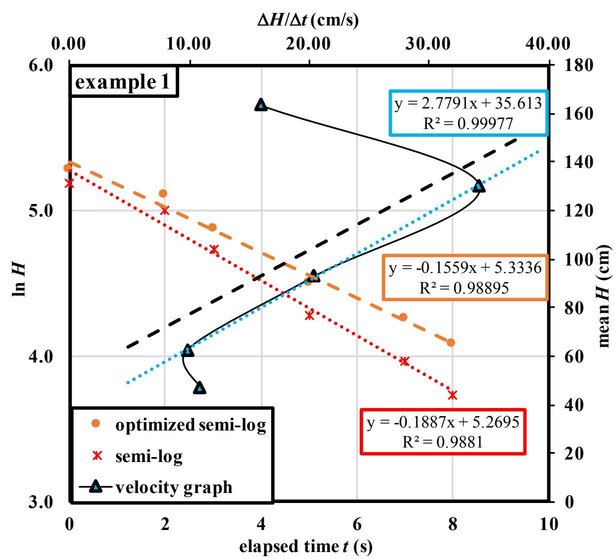

Figure 1. Example 1 in sand, L=225cm, D=11.4 cm

It is observed from Figure 1 that the test data pass through a nearly straight semi-log graph, which yields K_{VH1} of 9.9 x 10^{-3} cm/s. The velocity graph appears scattered instead of straight, and the R^2 of its best fit (the black dashed line) is 0.3, which provides an incorrect K_{VH2} of 2.0 x 10^{-2} cm/s. We selected the three points that form a linear line (the blue dotted line) to calculate the piezometric error H_0 and K'_{VH2}, which are 35.6 cm and 1.9 x 10^{-2} cm/s respectively. However, the Z-t method gives a different H_0 of -17.6 cm and the optimized hydraulic conductivity of K_{VH3} = 8.2 x 10^{-3} cm/s, which is considered to be the most accurate compared to the other K_{VH} values. It is obvious that the three K_{VH} values are different and the value of K_{VH3} is 213% larger than K_{CH}.

3.2 Example 2

The screen of the MW is also 305 cm in length and 360 cm was immersed. The groundwater was sampled for 32 minutes at a rate of 32.44 L/min and reached a constant head difference of 220.4 cm. The calculated K_{CH} is 4.5 x 10^{-3} cm/s. The recovery test data are illustrated in semi-log and velocity graphs in Figure 2.

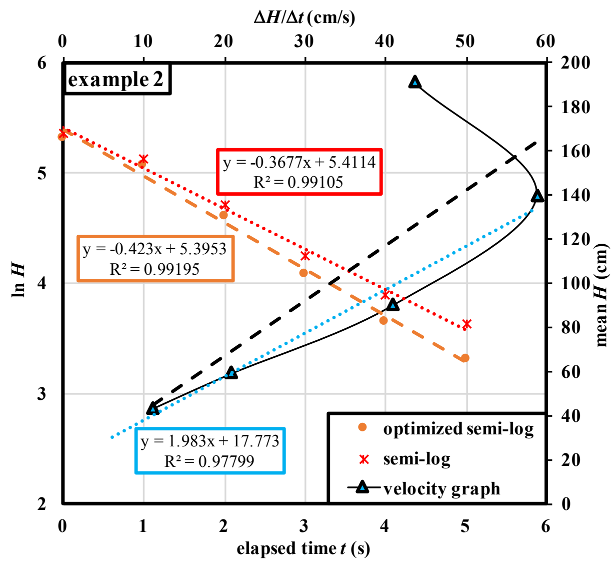

Figure. 2 Example 2 in sand, L=360cm, D=11.4cm

The semi-log plot is also a straight line, giving a K_{VH1} of 1.4 x 10^{-2} cm/s. The optimized one is more accurate, from which the K_{VH3} is equal to 1.6 x 10^{-2} cm/s with a peizometric correction of 10.3 cm. The velocity graph appears to have a similar shape to that shown in Figure 1, but without the last point being abnormal. It also has a bad linear fit (the black dashed line) with R^2 = 0.6, which determines a K_{VH2} of 1.5 x 10^{-2} cm/s. The last four points of the velocity graph has a better linear fit, where K'_{VH2} = 1.9 x 10^{-2} cm/s. From this, we can see that the K_{VH} and K_{CH} values are not in the same order, with the he K_{VH3} being greater than the K_{CH} by 249%.

3.3 Example 3

The length of the MW screen is 305 cm, and 298 cm was immersed. Compared to the examples 1 and 2, a smaller H_c of 3.7 cm was generated due to a lower Q of 5.03 L/min. The estimated K_{CH} is 4.8 x 10^{-2} cm/s. The water level started to recover after 15 minutes discharging, which were registered against time (plotted in Figure 3).

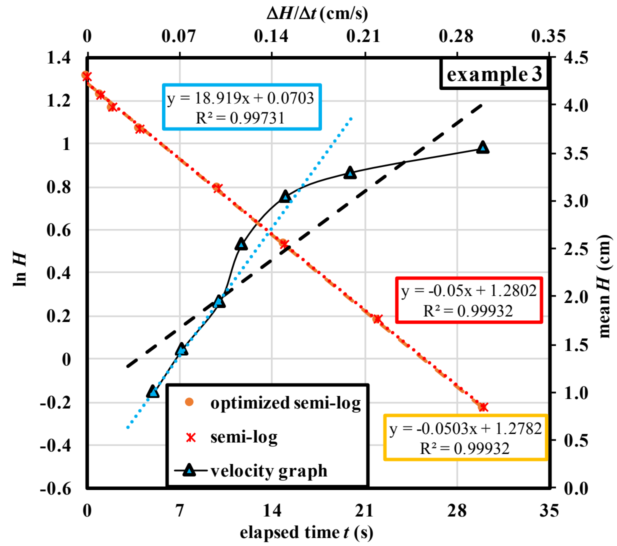

Figure. 3 Example 3 in sand, L=298cm, D=11.4 cm

In this case, the semi-log plot is perfectly linear and no piezometric error exists according to the *Z-t* method. Therefore, K_{VH1} = K_{VH3} = 2.1 x 10^{-3} cm/s. However, the velocity graph is downwardly curved and has a best fit line (the black dashed line), of which R^2 = 0.8 and K_{VH2} = 4.2 x 10^{-3} cm/s. The last three points pass through a straight portion that yield a K'_{VH2} of 2.3 x 10^{-3} cm/s, which is similar to the K_{VH1} and K_{VH3} values. However, the K_{VH3} is 95% lower than K_{CH}.

3.4 Example 4

The screen of the MW is 367 cm in length. There was a very long pumping duration before the recovery, but no information about the pumping rate and time were provided. Thus, the K_{CH} is unknown, and only K_{VH} values are obtained from the recovery data.

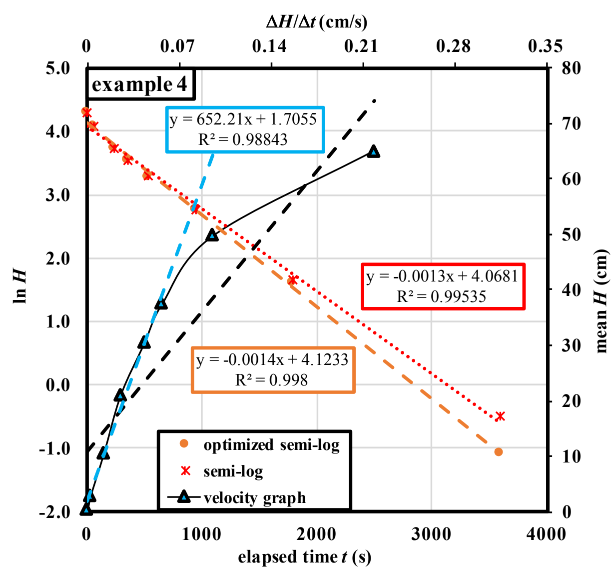

Figure. 4 Example 4 in till, L=367cm, D=10.16cm

In Figure 4, the original and optimized semi-log graphs are close, and thus yield similar K_{VH1} and K_{VH3} of 1.2 x 10^{-5} cm/s and 1.4 x 10^{-5} cm/s, respectively. The entire velocity data has a linear fit of R^2 = 0.8, giving K_{VH2} = 3.2 x 10^{-5} cm/s. From the straight portion of the late velocity data, a more accurate K'_{VH2} of 1.4 x 10^{-5} cm/s is obtained, which is equivalent to the optimized K_{VH3}.

3.5 Example 5

The same information was provided for this example as was provided for the example 4. Thus, the K_{CH} is unknown, and only the recovery data are plotted in Figure 5.

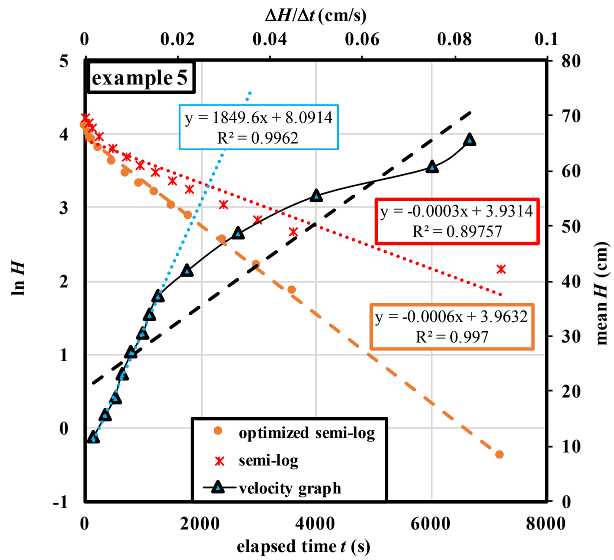

Figure. 5 Example 5 in till, L=367cm, D=10.16cm

The original semi-log plot in Figure 5 presents a larger curvature compared to other examples, thus its K_{VH1} is the most inaccurate at 2.8 x 10^{-6} cm/s. It was optimized to be straight by the *Z-t* method, which resulted in a K_{VH3} value of 5.7 x 10^{-6} cm/s. The shape of the velocity graph is similar to that of example 4, from which K_{VH2} = 1.6 x 10^{-5} cm/s. The K'_{VH2} value is 5.1 x 10^{-6} cm/s from the straight portion of the velocity graph, which is close to the K_{VH3}.

3.6 Discussion

The five examples illustrate that the original semi-log graphs are approximately straight except that the example 5 has an obvious upward curvature. They are optimized by the *Z-t* method in a spreadsheet to determine more accurate K_{VH3} values compared to the K_{VH1} values. Even with the optimization, the K_{VH3} values of examples 1 and 2 are over 200% higher than the corresponding K_{CH} values, and K_{VH3} of example 3 is 95% lower than its K_{CH} value.

Additionally, the shapes of velocity graphs are divided into two types: being scattered in examples 1 and 2, and downwardly curved in examples 3 to 5 instead of straight lines. The K_{VH2} values determined by the entire velocity graph differ from the K_{VH3} values. The early data of the velocity plot refers to recovery in the pipe, therefore the straight portions of the late data represent the recovery in the aquifer which are used to derive the H_0 and K'_{VH2}. In examples 3, 4 and 5, the derived H_0 values are close to those determined by the *Z-t* method, and the values of K'_{VH2} are very close to the K_{VH3} values. It is, however, not the case for examples 1 and 2. The reason might be the large pumping rate of the first two examples. The high flow rate may cause turbulence close to the screen, which enhances the energy dissipation, and thus generates a more important head loss and a large dewatering of the screen during pumping. Additionally, the K'_{VH2} from the straight portion is approximately equal to K_{VH3}, but still differs greatly from the K_{CH} values for example 3.

Based on the known condition of examples 1 and 3, that the screens were partially immersed, the deviations between the K_{CH} and K_{VH} values and the abnormal velocity plots are believed to be due to the poorly installed monitoring wells. However, this needs to be checked. Therefore, the results of CH recovery tests in another two MWs in good conditions are provided in the following section.

4 EXAMPLES OF GOOD WELLS

4.1 Example 6

Example 6 is a CH test conducted in the MW installed in a confined sand aquifer in Sorel. The MW was proved to be in good condition (Zhang et al. 2018b). The H_c is 15.7 cm, generated by a constant flow rate of 0.45 L/min, which yields a K_{CH} of 2.2 x 10^{-3} cm/s. The screen was entirely immersed during the test. The semi-log and velocity graphs of the recovery data collected after 17 minutes of pumping are plotted in Figure 6.

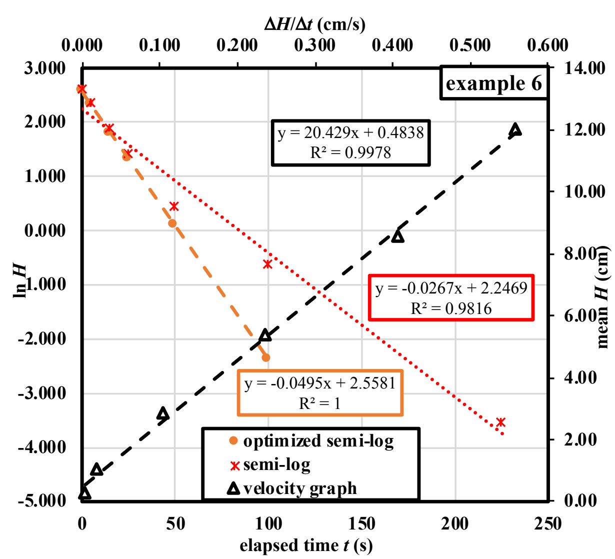

Figure. 6 Example 6 in sand, L=114cm, D=9cm.

The semi-log graph is slightly curved, and K_{VH1} = 1.1 x 10^{-3} cm/s. After optimization, the K_{VH3} has a value of 2.1 x

10^{-3} cm/s, which is very close to the previously calculated K_{CH}. The velocity plot is a straight line with an intercept on the y-axis of 0.48 cm, which is close to the H_0 of 0.45 cm achieved by the *Z-t* method. The K_{VH2} from the velocity graph is 2.1 x 10^{-3} cm/s, equivalent to K_{VH3}.

4.2 Example 7

Example 7 presents a CH test in the MW in a unconfined sand aquifer modelled with the numerical code, and thus the well is in good condition during a pumping period of 30 min. The screen was entirely immersed during the test. The H_c is 100 cm, generated by constant pumping of 36.5 L/min, which yielded a K_{CH} of 2.5 x 10^{-2} cm/s.

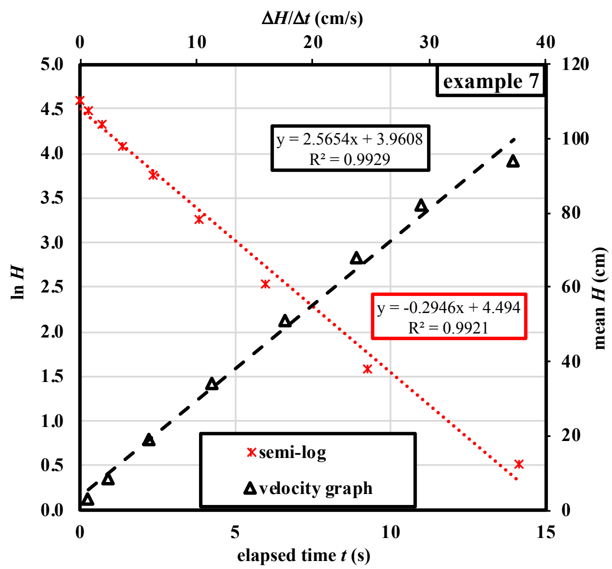

Figure. 7 Example 7, L=100cm, D=15.24cm.

The semi-log and the velocity graphs in Figure 7 are straight lines. No optimization is needed in this case. The K_{VH1} = K_{VH3} which is 2.5 x 10^{-2} cm/s, equivalent to the K_{CH}. The K_{VH2} is 3.2 x 10^{-2} cm/s, close to the K_{CH} value. It is noted that although the flow rate is higher compared to examples 1 and 2, the velocity plot is not scattered, because the hydraulic conductivity of the sand in example 7 is one order of magnitude higher than that in examples 1 and 2, and thus a higher flow rate is needed to generate the head difference.

5 CONCLUSION

Seven recovery data sets from CH tests are analyzed as if they were VH tests. They seem like plausible VH tests with water level changing smoothly back to the initial level, however, there are long pumping durations before the recovery (not a sudden water volume change). Therefore, the paper theoretically proved that the Hvorslev's semi-log and velocity plots used to interpret the VH test can also be applied also apply to the CH recovery test.

If the MW is perfectly installed and the CH test operation is good, the velocity graph of the recovery data appears to be straight, and the yielded K_{VH} values are close to the K_{CH} value, like what was obtained with good examples 6 and 7.

The examples 1, 2 and 3 show approximately straight Hvorslev's semi-log plots, but the derived K_{VH1} values from the original plot have around 1 order difference from the K_{CH} value. After the optimization of the semi-log graph, the K_{VH3} values of examples 1 and 2 are still greatly different from the corresponding K_{CH} values.

Two shapes of velocity graphs were observed in the poorly installed/test MWs. They are either scattered for examples 1 and 2 or downwardly curved for examples 3-5, which are difficult to analyze. In all cases, the values of K_{VH2} interpreted directly from the linear fitting lines of the entire velocity plots deviate from the K_{VH3} values. The H_0 and K'_{VH2} are obtained from the straight portion formed by late data. For examples (3-5) which have low flowrates, there are two results that need to be noted. Firstly, the H_0 values are similar to those estimated through the *Z-t* method. Secondly, the K'_{VH2} values are very close to the K_{VH3} values. However, these two results are false for the examples 1 and 2. The scattered shapes of the velocity graphs and discordant results are considered to be due to the high pumping rate, which may have created high parasitic head losses against the screen. All results of the MWs are gathered in Table 2.

Table 2. Elements of comparison for the seven examples.

example no.	1	2	3	4	5	6	7
flow rate	high	high	low	low	low	low	high
semi-log plot	straight	straight	straight	straight	slightly curved	slightly curved	straight
velocity plot	scattered	scattered	curved	curved	curved	straight	straight
K_{CH} (cm/s)	2.62x10^{-3}	4.50x10^{-3}	4.79x10^{-2}	--*	--*	2.18x10^{-3}	2.50x10^{-2}
K_{VH1} (cm/s)	9.94x10^{-3}	1.37x10^{-2}	2.14x10^{-3}	1.22x10^{-5}	2.77x10^{-6}	1.13x10^{-3}	2.54x10^{-2}
K_{VH2} (cm/s)	1.99x10^{-2}	1.49x10^{-2}	4.21x10^{-3}	3.24x10^{-5}	1.57x10^{-5}	2.06x10^{-3}	3.17x10^{-2}
K_{VH2}' (cm/s)	1.90x10^{-2}	1.87x10^{-2}	2.26x10^{-3}	1.44x10^{-5}	5.09x10^{-6}	2.06x10^{-3}	3.17x10^{-2}
K_{VH3} (cm/s)	8.21x10^{-3}	1.57x10^{-2}	2.15x10^{-3}	1.36x10^{-5}	5.68x10^{-6}	2.09x10^{-3}	2.54x10^{-2}
K_{VH3}/K_{CH}	3.13	3.49	0.04	--	--	0.96	1.02
comments	1-5: non-straight velocity plot and $K_{CH} \neq K_{VH3}$ indicates poorly-installed MWs * The flow rates were unknown, and thus K_{CH} could not be calculated.					6-7: good MWs	

In summary, the interpretation methods of VH tests are applicable to the recovery phase of CH tests based on the theoretical and experimental examinations. They can be used in combination with the Lefranc's solution for steady state, to check the general performance of the screen by comparing the K_{VH} with the K_{CH}. Even if the Hvorslev's plot seems to be linear, it is recommended to optimize the original semi-log graph and plot the velocity graph. If a great difference between K_{VH} and K_{CH}, and the velocity is not straight, it must be indicative of poor design or installation of the well or improper manipulation of the test, e.g., the screen is partially immersed, the water is dewatering down to the screen, the head losses is important close to the screen, etc..

REFERENCE

ASTM D4044. 2015. Standard Test Method (Field Procedure) for Instantaneous Change in Head (Slug) Tests for Determining Hydraulic Properties of Aquifers. *Annual Book of Standards*, Vol. 04. 08. ASTM International, West Conshohocken, Penn.

CAN/BNQ 2501-135. 2014. Soils - Determination of Permeability by The Lefranc Method, National Standard of Canada, Ottawa.

Cassan, M. 2005. *Les Essais de Perméabilité sur Site dans La Reconnaissance des Sols*. Presses des Ponts.

Chapuis R.P. 1998. Overdamped Slug Test in Monitoring Wells: Review of Interpretation Methods with Mathematical, Physical and Numerical Analysis of Storativity Influence. *Canadian Geotechnical Journal*. 35(5): 697–719.

Chapuis, R.P. 2015. Overdamped Slug Tests in Aquifers: The Three Diagnostic Graphs for A User - Independent Interpretation. *Geotechnical Testing Journal*.;38(4): 474–489.

Chapuis, R.P. 2017. Stress and Strain Fields for Overdamped Slug Tests in Aquifer Materials, and Resulting Conservation Equation. *International Journal for Numerical and Analytical Methods in Geomechanics*, 41(18): 1908-1921.

Chapuis, R.P., Paré, J.J. et Lavallée, J.G. 1981. Essais de perméabilité à niveau variable. *Proceedings, 10th ICSMFE*, Stockholm, Balkema, Vol. 1, pp. 401–406.

Chiasson, P. 2005. Methods of interpretation of borehole falling-head tests performed in compacted clay liners. *Canadian Geotechnical Journal*, 42(1): 79-90.

Hvorslev, M.J. 1951. Time-lag and Soil Permeability in Ground Water Observations. U.S. Army Engineering Waterways Experimental Station, Vicksburg, Miss., Bulletin 36.

ISO 22282-2. 2012, Geotechnical Investigation and Testing - Geohydraulic Testing - Part 2: Water Permeability Tests in a Borehole Using Open Systems, International Organization for Standardization, Geneva, Switzerland.

Lefranc, E. 1936. Procédé de Mesure de La Perméabilité des Sols dans Les Nappes Aquifères et Application au Calcul du Débit des Puits. *Le Génie Civil*, CIX(15): 306- 308.

Lefranc, E. 1937. La Théorie des Poches Absorbantes et Son Application à La Détermination du Coefficient de Perméabilité en Place et au Calcul du Débit des Nappes d'Eau. *Le Génie Civil*, CXI(20): 409-413.

Zhang, L., Chapuis, R.P., and Marefat, V. 2018a. Field Permeability Tests: Importance of Calibration and Synchronous Monitoring for Barometric Pressure Sensors. *Geotechnical Testing Journal*, in print.

Zhang, L., Chapuis, R.P., and Marefat, V. 2018b. Field Permeability Tests with Inward and Outward Flow in Confined Aquifer. *Geotechnical Testing Journal*, under review.